Selective heating mechanism of magnetic metal oxides by a microwave magnetic field

Motohiko Tanaka,[1] Hirohiko Kono,[2] and Koji Maruyama[3]
[1]*Coordination Research Center, National Institute for Fusion Science, Toki 509-5292, Japan*
[2]*Graduate School of Science, Tohoku University, Sendai 980-8578, Japan*
[3]*Advanced Science Institute, RIKEN, Wako 351-0198, Japan*
(Received 17 December 2008; revised manuscript received 13 February 2009; published 20 March 2009)

The mechanism of rapid and selective heating of magnetic metal oxides under the magnetic field of microwaves which continues beyond the Curie temperature T_c is identified by using the Heisenberg model. Monte Carlo calculations based on the energy principle show that such heating is caused by nonresonant response of electron spins in the unfilled 3*d* shell to the wave magnetic field. Small spin reorientation thus generated leads to a large internal energy change through the exchange interactions between spins, which becomes maximal around T_c for magnetite Fe_3O_4. The dissipative spin dynamics simulation yields the imaginary part of the magnetic susceptibility, which becomes largest around T_c and for the microwave frequency around 2 GHz. Hematite Fe_2O_3 with weak spontaneous magnetization responds much less to microwaves as observed in experiments. The heating of titanium oxide by microwave magnetic field only when oxygen defects are present is also explained by our theory in terms of the appearance of spontaneous magnetization.

DOI: 10.1103/PhysRevB.79.104420 PACS number(s): 78.70.Gq, 75.10.Hk, 81.20.Ev

I. INTRODUCTION

Microwave sintering is the process in which electromagnetic energy of microwaves is delivered directly to electrons or atoms in materials. It enables rapid heating that leads to melting and recrystallization of original solid matter. A laboratory experiment demonstrated that a grained magnetite sample was heated to above 1300 °C within a minute by applied microwaves.[1] The amount of energy consumption can be reduced and the release of CO_2 gas can be halved in the microwave iron making which reduces energy and environmental problems in modern iron industry.[2] Later, it was shown that various metallic oxides including magnetite and titanium oxide with oxygen defects TiO_{2-x} ($x>0$) were sintered quickly at the magnetic field maximum (i.e., the electric field null) in the microwave cavity experiments.[3] The product sintered in the microwave magnetic field was shown to have good magnetic properties as magnets.

The sintering of magnetite-hematite powders of micron sizes is characterized by selective heating. Only the domain of magnetite Fe_3O_4 with strong magnetization was heated to 1300 °C in the microwave magnetic field,[4] which is much above the Curie temperature T_c (585 °C). The adjacent domain of hematite Fe_2O_3 remained at low temperatures. The microwave sintering of magnetic materials is a nonresonant process that occurs with or without a static magnetic field and for any amplitude of wave magnetic field at a fixed microwave frequency. With ferromagnetic metals, microwave resonance absorption[5] and the nonresonant bolometric effect on dc resistance[6–8] were observed in ferromagnetic resonance (FMR) experiments under microwaves. These phenomena required a static magnetic field of specific strength to have resonance with microwaves, and were observed mainly below room temperature, which are attributed to Joule heating or eddy current. The microwave sintering, which occurs under wide range of strength and frequency of microwave magnetic field without a static magnetic field is physically a different process from the FMR process.

To date, the heating of dielectric materials by the microwave electric field was extensively studied.[9] We examined the heating of water, salt-contained water, and ice by microwaves using molecular-dynamics simulation.[10,11] The heating was attributed, respectively, to excitation of electric dipoles, the Joule heating of salt ions, and the weakening of the hydrogen-bonded H_2O network by the presence of salt ions. (Pure ice was not heated by 2.5 GHz microwave due to tight hydrogen bonds of water molecules.) For bulk metals, microwaves are reflected at the surface due to skin effects and do not transfer energy, while they penetrate into grained metallic powders (10 μm in diameter) for a few centimeters and heat them.[12] However, the sintering mechanism of metal oxides that have spontaneous magnetization under the magnetic field of microwaves has not been resolved.

In this paper, we show theoretically that the sintering of particles of magnetic metal oxides, including magnetite and titanium oxide with oxygen defects, by a microwave magnetic field is due to nonresonant response of electron spins in the unfilled 3*d* shell. We first use the energy principle and perform the Monte Carlo simulations. A small spin perturbation in response to an alternating external magnetic field results in a large internal energy change through exchange interactions. Next, studies in the time domain are done by performing dissipative spin dynamics simulation and detecting the linear response of spins. The temperature and frequency dependence of the heating rate by the microwave magnetic field is obtained on the basis of the imaginary part of magnetic susceptibility χ_i. These results agree well with those by the energy principle, and χ_i quantitatively accounts for the rapid heating of magnetite in the sintering experiments.

II. NUMERICAL PROCEDURES

We have used the following procedures in our numerical simulations. The magnetization of magnetite and hematite is well described by the Heisenberg model above the Verwey

transition temperature (120 K) (Ref. 13) since electrons are roughly localized.[14] The internal energy U of the magnetic system is represented by the three-dimensional spin vector $\mathbf{s}_i$ of the electron at the ith site, the exchange interaction coefficient J_{ij} between the ith and jth sites, and the external magnetic field $\mathbf{B}_w$ of microwaves, which reads

$$U(\mathbf{B}_w) = -\sum_{i,j} J_{ij}\mathbf{s}_i \cdot \mathbf{s}_j + \sum_i g\mu_B \mathbf{s}_i \cdot \mathbf{B}_w. \quad (1)$$

The summation of the exchange interactions in the first term is taken over the pairs of nearest-neighbor sites. The magnitude of the spin vector satisfies $|\mathbf{s}_i| = S$ for the spin angular momentum S. The second term, which may be called the Zeeman term, is the scalar product of magnetization $\mathbf{M} = -\Sigma_i g\mu_B \mathbf{s}_i$ and the magnetic field, $-\mathbf{M}\cdot\mathbf{B}_w$, where $g \cong 2$ and $\mu_B = e\hbar/2mc$. We note that the Weiss field (the internal magnetic field) is $B_{\text{Weiss}} \cong n_B J_{AB} S/g\mu_B \cong 240$ T, which is much larger than that of microwaves, where $n_B \cong 4.1$ is the effective magneton number of magnetite and J_{AB} is of a few meV. We also note that the individual spin interaction energy $J_{AB}S^2 \cong 0.016$ eV is comparable to the thermal energy at room temperature 0.026 eV. Thus, thermal effects are significant in the sintering process for which temperatures are much above 300 K.

To obtain a thermally equilibrated state, we minimize the internal energy of the spin system Eq. (1) at a given temperature using the Monte Carlo method with the Metropolis criterion. A trial random rotation is exerted on one of the spins in the nth step: the trial is accepted if the internal energy decreases $\delta U = U^n - U^{n-1} < 0$, or if the energy increase satisfies $\exp(-\delta U/k_B T) > \varepsilon$, where ε is a random number uniformly generated in the (0,1) interval, k_B is the Boltzmann constant and T is temperature; otherwise the trial is rejected.

To proceed further, we have to specify the crystal structure and the exchange interaction coefficients. For magnetite, the unit cell is a cubic box with the sides of 0.8396 nm at room temperature[15] and contains 24 irons: 16 of them are Fe^{3+} $(3d^5, S=5/2)$ and occupy all the tetrahedral sites (A site, eight positions) and half of the octahedral sites (B site). The rest of irons are eight Fe^{2+} $(3d^6, S=2)$, and are located at B sites. The exchange interaction coefficients are all negative and satisfy $|J_{AB}| > |J_{AA}|, |J_{BB}|$.[14] We assume $J_{AB} = -4.0$ meV and $J_{AA} = J_{BB} = -0.3$ meV, where the former is larger in magnitude than the theoretically estimated value 2.5 meV (Ref. 16) to reproduce T_c in our model.

III. RESULTS

Using the procedures described in Sec. II, we first calculate the equilibrated state without an applied magnetic field for the periodic crystal of magnetite with $3\times3\times3$ unit cells. Below T_c, spins are ordered along the c axis due to the exchange interactions, with the spins at A-sites and those at B-sites oriented oppositely. The temperature dependence of magnetization calculated with our model is shown in Fig. 1. The validity of our model is confirmed by the numerical result that the spontaneous magnetization decreases monotonically with temperature and vanishes above T_c, as expected. Our calculated value $M_c/M_0 \cong 1.1$ at 300 K roughly agrees with the experimental value $M_s/M_0 \cong 1.3$,[14] where $M_0 = N\mu_B$ with N as the number of irons in the system.

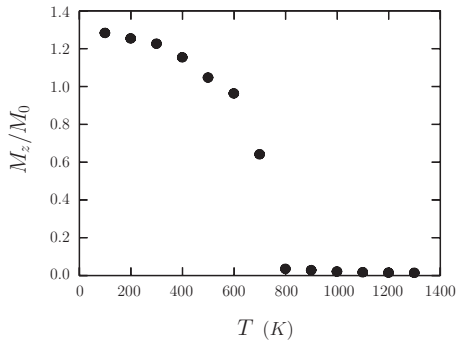

FIG. 1. Temperature dependence of the magnetization along the c axis (z axis), $M_z = -\Sigma_i g\mu_B s_{z,i}$, calculated by Monte Carlo simulation using the Heisenberg model for magnetite described in the text. The magnetization is normalized by $M_0 = N\mu_B$, where N is the number of Fe ions. The magnetization vanishes above the Curie temperature T_c of magnetite 858 K.

Next, we apply a slowly varying magnetic field $\mathbf{B}_w$ to the equilibrium obtained above, and perform the Monte Carlo simulation. The varying speed of the magnetic field is chosen to be slow enough for spins to relax to the state of an instantaneous magnetic field. The amplitude of the magnetic field is 1 T unless otherwise specified, which is still by 2 orders of magnitude less than the Weiss field. Spins relax in orientation under the magnetic field and the internal energy $U(\mathbf{B}_w)$ depends on the magnitude and orientation of $\mathbf{B}_w$. We evaluate the difference between the maximum and minimum of the internal energy during a period of the magnetic field change,

$$\Delta U^{(\text{mc})} = U^{(\text{mc})}_{\text{max}} - U^{(\text{mc})}_{\text{min}}. \quad (2)$$

Here, the superscript (mc) stands for "Monte Carlo" simulation. The energy ΔU that is to be released irreversibly to lattice atoms by dissipation process, possibly by spin-lattice interactions,[17] is obtained by subtracting from $\Delta U^{(\text{mc})}$ the reversible energy change, $\Delta U^{(\text{rev})} = U^{(\text{rev})}_{\text{max}} - U^{(\text{rev})}_{\text{min}}$. The latter is obtained by solving the spin dynamics equation without dissipation,

$$d\mathbf{s}_i/dt = \sum_j (2J_{ij}/\hbar)\mathbf{s}_i \times \mathbf{s}_j - (g\mu_B/\hbar)\mathbf{s}_i \times \mathbf{B}_w. \quad (3)$$

The energy difference ΔU can be used as the index of heating by the microwave magnetic field. This is verified later by agreement of the estimation based on the imaginary part of the magnetic susceptibility with the ΔU here and also the experimental value of the heating rate.

Figure 2 shows the changes in (a) the average magnetization in the z direction (c axis), (b) the total internal energy (solid line) and the contribution of the Zeeman term (dashed line) at 700 K against (c) the alternating magnetic field which is parallel to the c axis. In the present case, the magnetization M_z stays negative along the z axis, and the Zeeman term $-\mathbf{M}\cdot\mathbf{B}_w$ takes positive or negative value according to whether $\mathbf{B}_w$ is parallel or antiparallel to the c axis. In the phase where the applied magnetic field becomes more nega-

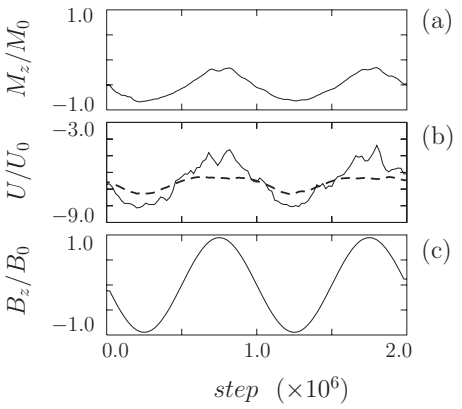

FIG. 2. Model calculation for the magnetic field effects on magnetite at 700 K. The changes in (a) the z component of magnetization $M_z=-\Sigma_i g\mu_B s_{z,i}$, (b) the internal energy U per Fe (solid line), and the contribution of the Zeeman term to the internal energy (dashed line, for which the zero baseline is shifted downward by $7U_0$) are shown against (c) the applied magnetic field B_z in the Monte Carlo simulation steps. The z axis is parallel to the c axis. The normalization factors are as follows: $M_0=N\mu_B$, $U_0=10^{-21}$ J, and $B_0=1$ T.

tive, the magnitude of magnetization increases due to alignment of spins parallel to the c axis, and the internal energy becomes minimal in this phase of the magnetic field. We note that the large change in the internal energy occurs through the exchange interactions because the energy associated with the Zeeman term is small and reversible, with the former by a factor of $J_{AB}S/g\mu_B B_w$ ($\geqslant 1$) larger than the latter, as depicted in Fig. 2(b). In fact, the contribution of the Zeeman term is small and roughly the same as that obtained with the dissipationless spin dynamics Eq. (3).

The distribution functions at the 1.25×10^6th Monte Carlo step in Fig. 2 are shown in Fig. 3. The x and z directions are taken along the a and c axes, respectively. In the x direction, the spins form centered Boltzmann distributions and no mag-

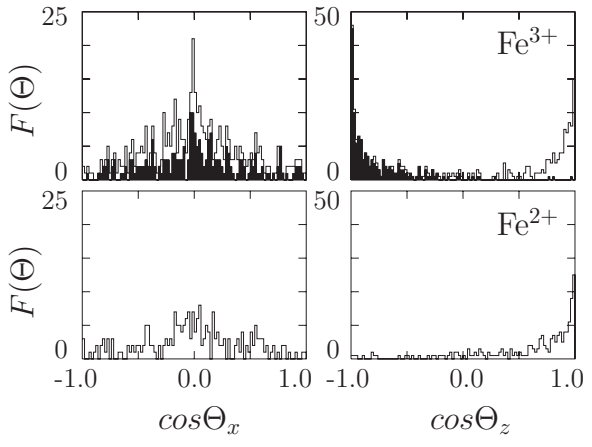

FIG. 3. The distribution functions of spins along the x direction (leftward panels) and z direction (rightward panels), Θ is the angle of the spin either with the x or z axis. The distribution functions in the upper panels correspond to Fe^{3+} (the shaded area denotes the states of spins at A sites) and those in the lower panels correspond to Fe^{2+}.

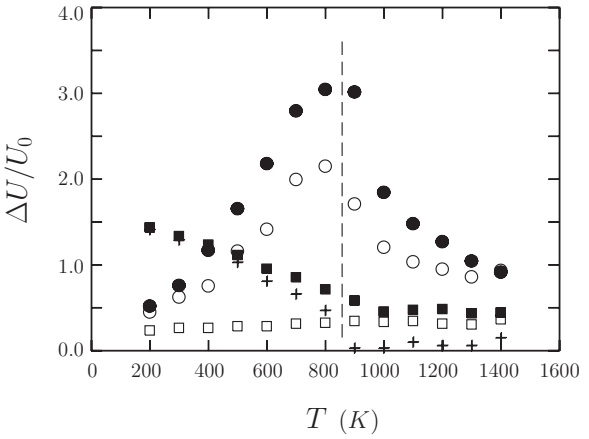

FIG. 4. Temperature dependence of the internal energy change (per Fe) during a period of an applied magnetic field of $B_w=1$ T ($U_0=10^{-21}$ J). The filled circles and squares correspond, respectively, to the irreversible energy difference ΔU and the change in the Zeeman term $\Delta(\mathbf{M}\cdot\mathbf{B}_w)$ for magnetite with the magnetic field parallel to the c axis; crosses correspond to $\Delta U^{(\mathrm{rev})}$ obtained by the spin dynamics of Eq. (3) which is reversible. The open circles and squares correspond to ΔU and the change in the Zeeman term, respectively, when the magnetic field is applied parallel to the a axis. The vertical line denotes T_c of magnetite.

netization occurs along this direction. (The shaded areas correspond to the Fe^{3+} at A sites.) Ferrimagnetization occurs along the z direction. The Fe^{3+} spins at A sites are antiparallel to the z axis and those of Fe^{2+} and Fe^{3+} at B sites are parallel to it. The change in the orientations in response to the microwave magnetic field is subtle, yet it gives rise to a maximum in the magnitude of magnetization periodically, as shown in Fig. 2(a).

Figure 4 shows the calculated temperature dependence of the internal energy difference $\Delta U=\Delta U^{(\mathrm{mc})}-\Delta U^{(\mathrm{rev})}$ when the microwave magnetic field is parallel either to the c axis (filled circles) or to the a axis of magnetite (open circles). The difference in the energy becomes largest when the polarization of the magnetic field is parallel to the c axis, and it increases linearly with temperature up to T_c. The change in the reversible energy $\Delta U^{(\mathrm{rev})}$ and that in the Zeeman term for the former case are shown by crosses and filled squares, respectively. The energy change $\Delta U^{(\mathrm{rev})}$ is similar to that in the spontaneous magnetization which decreases with temperature and vanishes above T_c. The change in the Zeeman term is almost the same as $\Delta U^{(\mathrm{rev})}$ but is finite for $T>T_c$. The Zeeman term in the Monte Carlo simulation remains finite because an induced magnetization appears synchronously with and along the magnetic field independently of its polarization in the paramagnetic regime. The major contribution to the internal energy difference ΔU is attributed to the exchange interactions since the change in the Zeeman term is reversible and thus almost subtracted in ΔU. The temperature dependences shown in Fig. 4 are in excellent agreement with the sintering experiments in the microwave magnetic field,[3,4] where the heating of magnetite was enhanced at 300–600 °C and continued to much above T_c.

An argument that involves time scales as well as the temperature dependence of heating is made possible by solving

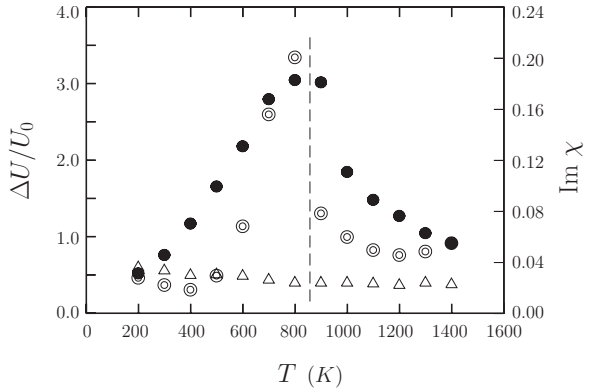

FIG. 5. Temperature dependence of the internal energy change (per Fe) ΔU for hematite is shown by triangles, and that of magnetite with the magnetic field parallel to the c axis is shown by filled circles as reference, for $B_w=1$ T ($U_0=10^{-21}$ J). The imaginary part of the magnetic susceptibility obtained by dissipative spin dynamics Eq. (4) for $\tau_D=1$ ns is shown by double circles (in mol^{-1}). The vertical line denotes T_c of magnetite.

the dissipative spin dynamics. Here, the term $-(\mathbf{s_i}-\mathbf{s_{i0}})/\tau_\mathbf{D}$ is added to the right-hand side of Eq. (3). Namely, we solve

$$d\mathbf{s}_i/dt = \sum_j (2J_{ij}/\hbar)\mathbf{s}_i \times \mathbf{s}_j - (g\mu_B/\hbar)\mathbf{s}_i \times \mathbf{B}_w - (\mathbf{s_i}-\mathbf{s_{i0}})/\tau_\mathbf{D}. \tag{4}$$

A set of $\mathbf{s_{i0}}$ constitutes the equilibrium spin distribution function for a given temperature and magnetic field under the Monte Carlo calculation. The imaginary part of the magnetic susceptibility χ_i is obtained from the linear response of magnetization against the applied alternating magnetic field. χ_i gives the heating rate $dT/dt \propto \chi_i$, and is shown for magnetite with double circles in Fig. 5. It peaks around 800 K and is consistent with ΔU obtained with the energy principle of the Monte Carlo calculation.

The dependence of the imaginary part of magnetic susceptibility χ_i on the relaxation time τ_D is shown in Fig. 6 for the 2.5 GHz microwave. We see that χ_i is inversely proportional to τ_D in the $\tau=2\pi/\omega \leq \tau_D$ range. Also, the dependence of χ_i on the microwave frequency is shown in Fig. 7 for $\tau_D=1$ ns. The imaginary part of magnetic susceptibility

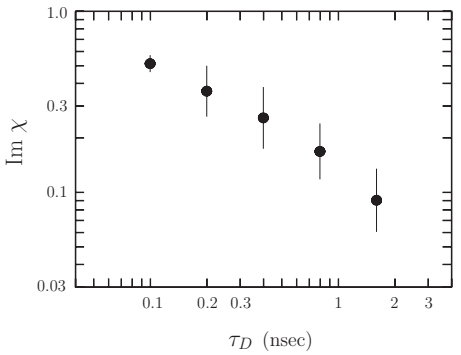

FIG. 6. The relaxation time τ_D dependence of the imaginary part of magnetic susceptibility χ (in mol^{-1}) for the 2.5 GHz microwave and temperature 700 K.

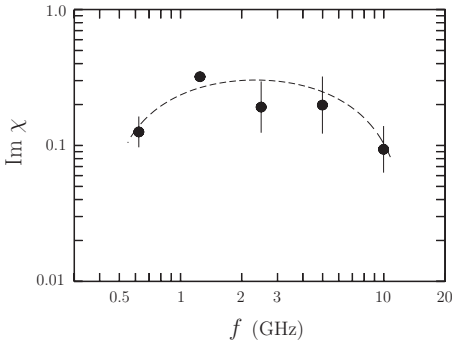

FIG. 7. The microwave frequency f dependence of the imaginary part of magnetic susceptibility χ (in mol^{-1}) for the relaxation time $\tau_D=1$ ns and temperature 700 K.

peaks around 2 GHz. This agrees with the experimentally deduced magnetic permeability for magnetite.[18] In our calculation, the relaxation time is assumed to be constant irrespectively of temperature or microwave frequency. However, if the relaxation time becomes small with temperature rise, the heating rate increases as τ_D^{-1} as shown in Fig. 5, resulting in more rapid heating at elevated temperatures.

From these data, one obtains the heating rate $dT/dt \sim (1/2)\omega\chi_i B_{\mathrm{mw}}^2/c_p \cong 300$ K/s for the case of $\tau_D=1$ ns and the microwave field $B_{\mathrm{mw}}=150$ G, where the heat capacity c_p is 210 J/K mol at 600 K (the wave period is 400 ps for the 2.45 GHz microwave). This is large enough to account for the experimental value $(dT/dt)_{\mathrm{ex}} \cong 250$ K/s in the microwave sintering of magnetite.[3]

The dependence of the internal energy change in magnetite per wave period on the applied magnetic field is shown in Fig. 8. The magnetic field amplitude ranges from 0.125 to 1.0 T. It is well fitted by the quadratic law B^2, therefore, ΔU, the heating rate is proportional to the microwave power.

Hematite has a different crystal structure from magnetite[15] and has weak spontaneous magnetization. The calculated change in the internal energy ΔU is plotted for various temperatures by triangles in Fig. 5. By comparison of ΔU with the case of magnetite, the response of hematite to the alternating magnetic field is considerably weak. This is consistent with the experimental fact that only the domain of magnetite in a magnetite-hematite composite powder was heated by the magnetic field of microwaves.[4]

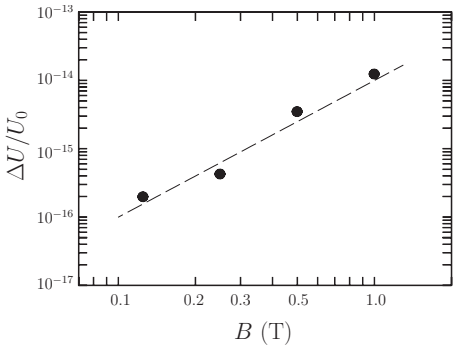

FIG. 8. Magnetic field dependence of the internal energy change in magnetite per wave period for the 2.5 GHz microwave and temperature 700 K. The dotted line corresponds to B^2.

The observation that heating of titanium oxide occurs only when oxygen defects are present,[19] TiO_{2-x} $(x>0)$, is explained in a similar fashion. Titanium in titanium oxide TiO_2 is a Ti^{4+} ion with $3d^0$ electron configuration, which has no electrons in the $3d$ shell. Thus, it has no spontaneous magnetization and should not respond to microwave magnetic field, similarly with hematite. However, when there are oxygen defects, the trivalent titanium ions Ti^{3+} appear which have $3d^1$ electron configuration. The spins of these $3d$ electrons respond to the magnetic field of microwaves, and absorb microwave energy which leads to observed heating under the microwave magnetic field.

IV. SUMMARY

In this paper, we have showed theoretically the mechanism of the rapid and selective heating of magnetic metal oxide particles by the magnetic field of microwaves. We adopt the Heisenberg model, and perform both Monte Carlo calculation and dissipative spin dynamics simulations. The heating occurs due to the response of magnetization to microwaves, which originates from electron spins residing in the unfilled $3d$ shell. Their nonresonant response causes a large change in the internal energy through the exchange interaction between spins, which is by a factor of $J_{AB}S/g\mu_B B_w$ $(\gg 1)$ larger than the Zeeman term. It persists above the Curie temperature T_c because each electron spin is able to respond to the alternating magnetic field of microwaves even above T_c. This energy change will then be dissipated to lattices and contribute to heating.

Hematite Fe_2O_3 which has only weak spontaneous magnetization shows much less response to microwaves than magnetite. Also, the heating of titanium oxide having oxygen defects TiO_{2-x} $(x>0)$ by the microwave magnetic field is explained by our theory in terms of intrinsic (spontaneous) magnetization.

The imaginary part of the magnetic susceptibility Im χ obtained by solving dissipative spin dynamics agrees well with the heating results by the Monte Carlo calculation. We have also presented the dependences of the heating rate on the frequency of microwaves and on the spin-relaxation time. These results well account for the large heating rate of magnetic metal oxide by the microwave magnetic field in the sintering experiments.

ACKNOWLEDGMENTS

One of the authors (M.T.) is highly grateful to M. Sato, R. Roy, D. Agrawal, and I. Ohmine for fruitful discussions. He also thanks M. Yamashiro and M. Ignatenko for careful reading of the manuscript. This work was supported by a Grant-in-Aid for Prime Area Research No. 18070005 from the Japan Ministry of Education, Science, and Culture.

[1] R. Roy, D. Agrawal, J. Cheng, and S. Gedevanishvili, Nature (London) **399**, 668 (1999).
[2] K. Ishizaki, K. Nagata, and T. Hayashi, ISIJ Int. **46**, 1403 (2006).
[3] J. Cheng, R. Roy, and D. Agrawal, Mater. Res. Innovations **5**, 170 (2002).
[4] M. Sato, A. Matsubara, K. Kawahata, O. Motojima, T. Hayashi, and S. Takayama, *Microwaves and High Frequency Heating* (AMPERE, Modena, Italy, 2005) pp. 277–280.
[5] L. R. Bickford, Phys. Rev. **78**, 449 (1950).
[6] S. T. Goennenwein, S. W. Schink, A. Brandlmaier, A. Boger, M. Opel, R. Gross, R. S. Keizer, T. M. Klapwijk, A. Gupta, H. Huebl, C. Bihler, and M. S. Brandt, Appl. Phys. Lett. **90**, 162507 (2007).
[7] Y. S. Gui, N. Mecking, A. Wirthmann, L. H. Bai, and C.-M. Hu, Appl. Phys. Lett. **91**, 082503 (2007).
[8] N. Biziere and C. Fermon, Appl. Phys. Lett. **92**, 092503 (2008).
[9] K. I. Rybakov, V. E. Semenov, S. V. Egorov, A. G. Eremeev, I. V. Plotnikov, and Yu. V. Bykov, J. Appl. Phys. **99**, 023506 (2006).
[10] M. Tanaka and M. Sato, J. Chem. Phys. **126**, 034509 (2007).
[11] M. Tanaka and M. Sato, J. Microwave Power Electromagn. Energy **42**, 62 (2008).
[12] M. Suzuki, M. Ignatenko, M. Yamashiro, M. Tanaka, and M. Sato, ISIJ Int. **48**, 681 (2008).
[13] J. R. Cullen and E. Callen, J. Appl. Phys. **41**, 879 (1970).
[14] C. Kittel, *Introduction to Solid State Physics*, 6th ed. (Wiley, New York, 1986), Chap. 15 and 16.
[15] N. I. M. S. Materials Database, Basic Crystal Structures, http://www.nims.go.jp/.
[16] R. E. Mills, R. P. Kenan, and F. J. Milford, Phys. Rev. **145**, 704 (1966).
[17] J. Fivez, Z. Phys. B: Condens. Matter **42**, 209 (1981).
[18] Y. Ma, V. K. Varadan, and V. V. Varadan, PIER **06**, 315 (1992).
[19] R. Peelamedu, M. Fleming, D. Agrawal, and R. Roy, J. Am. Ceram. Soc. **85**, 117 (2002).